Study of membrane deformations induced by Hepatitis C protein NS4B and its terminal amphipathic peptides

Malika Ouldali, Karine Moncoq, Agnès de La Croix de La Valette, Ana Arteni, Jean-Michel Betton, Jean Lepault

Version of Record: https://www.sciencedirect.com/science/article/pii/S0005273620303795
Manuscript_d577415232fe99f666ca80e0ef673384

Study of membrane deformations induced by Hepatitis C protein NS4B and its terminal amphipathic peptides

Malika Ouldali[1*], Karine Moncoq[2,3*], Agnès de la Croix de la Valette[1], Ana A. Arteni[1], Jean-Michel Betton[4] and Jean Lepault[1+]

[1]Institute for Integrative Biology of the Cell (I2BC), CEA, CNRS, Univ. Paris-Sud, Université Paris-Saclay, 91198, Gif sur Yvette, France
[2]Département de Virologie, Unité de Virologie Structurale, URA-CNRS 3015, Institut Pasteur, F-75724 Paris cedex 15, France.
[3]Univ Paris Diderot, Sorbonne Paris Cité, Laboratoire de Physico-Chimie Moléculaire des Membranes Biologiques, UMR 7099, CNRS, Institut de Biologie Physico-Chimique, 13 rue Pierre et Marie Curie, 75005 Paris, France
[4]Unité de Biochimie Structurale, URA-CNRS 2185, Institut Pasteur, 75724 Paris cedex 15, France.

[*] Contributed equally to this work
[+]To whom corresponding should be addressed:
Jean Lepault
I2BC du CNRS
Avenue de la Terrasse
F-91198 Gif sur Yvette, France
33 (0)6 09 79 38 12
jean.lepault@orange.fr

KEYWORDS: HCV-NS4B induced membrane disorder; NS4B peptides induced membrane perforation; one NS4B peptide induced membrane fusion; Cryo-EM of membranes disordered by NS4B; CryoEM of membranes fused by NS4B peptide

ABSTRACT

Many viruses destabilize cellular membranous compartments to form their replication complexes, but the mechanism(s) underlying membrane perturbation remains unknown. Expression in eukaryotic cells of NS4B, a protein of the hepatitis C virus (HCV), alters membranous complexes and induces structures similar to the so-called membranous web that

appears crucial to the formation of the HCV replication complex. As over-expression of the protein is lethal to both prokaryotic and eukaryotic cells, NS4B was produced in large quantities in a “cell-free" system in the presence of detergent, after which it was inserted into lipid membranes. X-ray diffraction revealed that NS4B modifies the phase diagram of synthetic lipid aqueous phases considerably, perturbing the transition temperature and cooperativity. Cryo-electron microscopy demonstrated that NS4B introduces significant disorder in the synthetic membrane as well as discontinuities that could be interpreted as due to the formation of pores and membrane merging events.

C- and N-terminal fragments of NS4B are both able to destabilize liposomes. While most NS4B amphipathic peptides perforate membranes, one NS4B peptide induces membrane fusion. Cryo-electron microscopy reveals a particular structure that can be interpreted as arising from hemi-fusion-like events. Amphipathic domains are present in many proteins, and if exposed to the aqueous cytoplasmic medium are sufficient to destabilize membranes in order to form viral replication complexes. These domains have important functions in the viral replication cycle, and thus represent potential targets for the development of anti-viral molecules.

HIGHLIGHTS

-NS4B of hepatitis C virus disorders biological membranes.

-The phase transitions of aqueous synthetic lipid phases lose cooperativity when NS4B is present.

-One of the four terminal amphipathic domains is shown sufficient to perforate and fuse membranes.

CryoEM of membranes fused by NS4B peptide reveals a structure that can be interpreted as arising from multi-hemi-fusion-like events.

INTRODUCTION

All positive-stranded RNA (+RNA) viruses modify host cytoplasmic membrane complexes, and these altered structures appear important for viral genome replication (reviewed in [1]) – although the mechanism(s) of membrane perturbation remains poorly understood. Some DNA and double-stranded RNA viruses (poxviruses, reoviruses respectively) also present a membrane-associated replication complex. To better characterize the membrane deformations induced by viruses, we studied a known active membrane protein, NS4B of the hepatitis C virus (HCV).

HCV is a major cause of chronic liver disease, with approximately 3 % of the world population infected [2]. Discovered more than twenty years ago [3], HCV is an enveloped +RNA virus belonging to the genus Hepacivirus of the Flaviviridae family. The HCV genome (ca 9.6 kb) consists of a single open reading frame (ORF) flanked by 5' and 3' untranslated regions (UTRs). The ORF encodes a polyprotein that is processed by cellular and viral proteases to generate the structural (core, E1 and E2) and non-structural (NS) proteins. NS proteins are involved both in viral particle maturation/secretion (NS1 or p7, and NS2) and viral genome replication (NS3, NS4A, NS4B, NS5A and NS5B) (reviewed in [4]).

Formation of the HCV replication complex (RC) is associated with large cytoplasmic membrane rearrangements, anchoring and protecting the RC to facilitate efficient replication [5]. These altered membranes, believed to be derived from the endoplasmic reticulum (ER), are constituted of small vesicles embedded in a membranous matrix of circular or undulating membranes, constituting a rather compact structure referred to as the membranous web (MW) [6]. Similar rearrangements have been described in the livers of HCV-infected patients [7]. The NS proteins have been immunolocalized in the MW [6] revealing the formation of intense cytoplasmic membrane-associated foci (MAF) where NS proteins are also localized [8].

Despite the considerable amount of information available on the viral proteins involved in RC and MW (reviewed in [4, 9-11]), the mechanism of their formation is not yet fully understood. It is likely that cellular factors act in this process - indeed, a growing number of host factors have been identified as components of the MW, which are also required for HCV replication (see [12] for a review).

The presence and accumulation of NS proteins upon their synthesis in the ER is the first step in formation of the RC. In particular, it has been shown that MW or MAF specifically appear upon over-expression of NS4B [6, 8]. This suggests that NS4B is a possible triggering factor of MW formation. NS4B is a 27 kDa integral membrane protein [13] composed of three

domains: the cytosolic N- and C-termini, and a central transmembrane domain comprising 4 to 5 helices [8]. Each cytosolic domain contains 2 amphipathic helices, the N-terminal AH1 and AH2 [14, 15], and the C-terminal H1 and H2 [16]. Studies on isolated peptides corresponding to these amphipathic helices revealed their ability to interact with and perturb model and cellular membranes [17-21]. Both N- and C terminal domains, as well as an homo-oligomerization of NS4B, are all thought to be linked to MW formation [22-24]. In addition, NS4B has been shown to bind nucleotides [25], to hydrolyze tri-nucleotides [26] and to bind RNA [27]. As a consequence of its apparent role in the replication process, NS4B has become a potential antiviral target (reviewed in [28]).

Data on NS4B-induced MW are only available in either a cellular context, or an artificial one involving isolated amphipathic peptides and liposomes [17, 29]. However, the precise intrinsic effect of NS4B on membranes remains to be determined. Our study aimed to determine the effect of NS4B on model membranes (liposomes). We produced large amounts of full-length NS4B in a cell-free expression system [30]. The purified protein was reconstituted into model membranes and further characterized by X-ray diffraction and cryo-electron microscopy (CryoEM). Our data demonstrate that NS4B destabilizes and fragments membrane vesicles. Peptides formed by the amphipathic helices present at the terminal extremities of NS4B are shown to perforate membranes and induce their fusion - in particular, they induce liposome hemi-fusion-like events. In conclusion, this study provides the first insights into the molecular mechanism of NS4B, and its involvement in cellular membrane reorganization and the formation of MW during HCV infection. Although numerous proteins participate in RC formation, membrane destabilization can be induced in the presence of hydrophobic domains or peptides only. The effects of NS4B on biological membranes can be generalized to all membrane-destabilizing proteins that contain amphipathic domains, whether in a viral or cellular context.

RESULTS

Protein expression and purification

Over-expression of the HCV NS4B gene (genotype 1a H77C) was lethal to E. *coli* (data not shown). The membrane protein was therefore produced using a cell-free expression system, in the presence of detergent to provide an hydrophobic environment. NS4B constructs were designed in fusion with a His-tag at either the N- or C-terminus (His-NS4B, NS4B-His respectively). Their expression was tested in small-scale batch mode in the presence of 1% Brij35, a detergent commonly used in cell-free expression. Although the two constructs of NS4B yielded a single band at the expected size (Figure SI 1A), only NS4B-His was detected by Western blot analysis using anti His-tag antibodies (Figure SI 1B). This suggests that the His-tag in His-NS4B is either hidden by the protein conformation or degraded, hampering correct antibody recognition – and also, potentially, its binding to the Ni-NTA column. Therefore, the C-terminally-tagged construct NS4B-His was preferred for large-scale production - referred to henceforth as NS4B. Brij35 was exchanged for DDM and the protein was used within a few days.

Visualization of the effects of NS4B on model membranes by cryo-electron microscopy (cryoEM)

Insertion of detergent-isolated membrane proteins in their native medium relies on detergent removal of a ternary aqueous solution containing three solutes: lipid, protein and detergent. Detergent removal can be achieved by either dialysis or BioBeads treatment (see[31]). Judged by the formation of liposomes in the absence of protein, both methods worked well (Figure SI 2). The resultant liposomes are, however, formed more rapidly with Biobeads (hours versus days), and displayed lower polydispersity (Figure SI 2). All experiments were therefore performed using BioBeads. The effects of NS4B on the structure of model membranes were analyzed at different lipid-to-protein molar ratios (LPR).

Membrane-reconstituted samples with or without the protein were first analyzed by conventional negative staining (Figure SI 2 and 3), and then by cryoEM in order to preserve the structure of aqueous lipidic phases [32] (Figure 1).

Pure lipid samples contained liposomes that were mostly multilamellar when observed by cryoEM (Figure 1A). In the presence of NS4B at molar lipid-to-protein ratios (LPR) of 500 or lower, NS4B affected the morphology of the liposomes in a concentration-dependent manner (Figure 1 B, C and D). The lower the LPR, the more heterogeneous and disordered the membranes appeared (see Figure 1B and 1C). For LPR lower than 50, no liposomes were

present at all – instead, small objects were observed consistent with the presence of lipid micelles (Figure 1D). While the exact structure of these objects is unknown, lipid micelles surrounding protein molecules represent a reasonable hypothesis. Figure 2 shows enlarged areas of figure 1. In the absence of NS4B, the membranes are parallel and their double-layered structure is clearly visible (Figure 2A). For increasing ratios of NS4B, membranes become more locally curved and fewer double-layered structures are observed (Figures 2B and 2C). Due to the low molecular weight of the protein (27kDa), the micelles containing NS4B exhibit low contrast (figure 2D). These observations suggest that NS4B possesses the ability to disorganize membranes by imposing local constraints that alter membrane curvature. Similar results were obtained with liposomes of different composition (soybean phosphatidyl-choline, synthetic lecithine such as dimerystoyl-phosphatidyl-choline (DMPC); data not shown). Further experiments were carried out at LPR between 100 and 300, corresponding to the region of major membrane alterations.

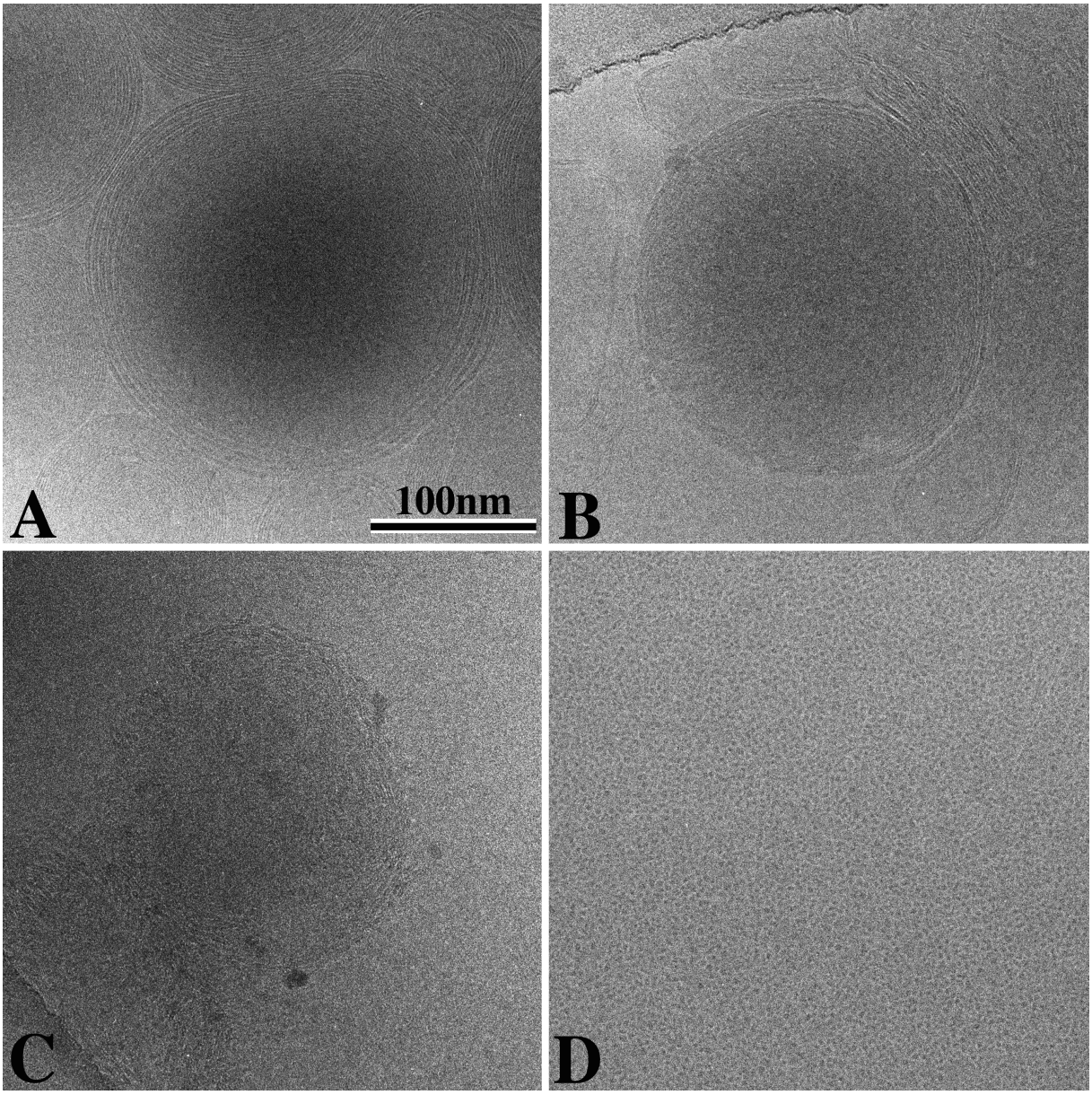

Figure 1: CryoEM. Liposomes reconstituted at different lipid to NS4B protein ratio (LPR) and observed by cryo-EM. A no protein. B LPR=500. C LPR=100. D LPR=10. Pure liposomes show regular stacks of membranes. The more NS4B is present, the more the stacking is perturbed due to the membrane deformation imposed by NS4B and the less are the visualized membranes.

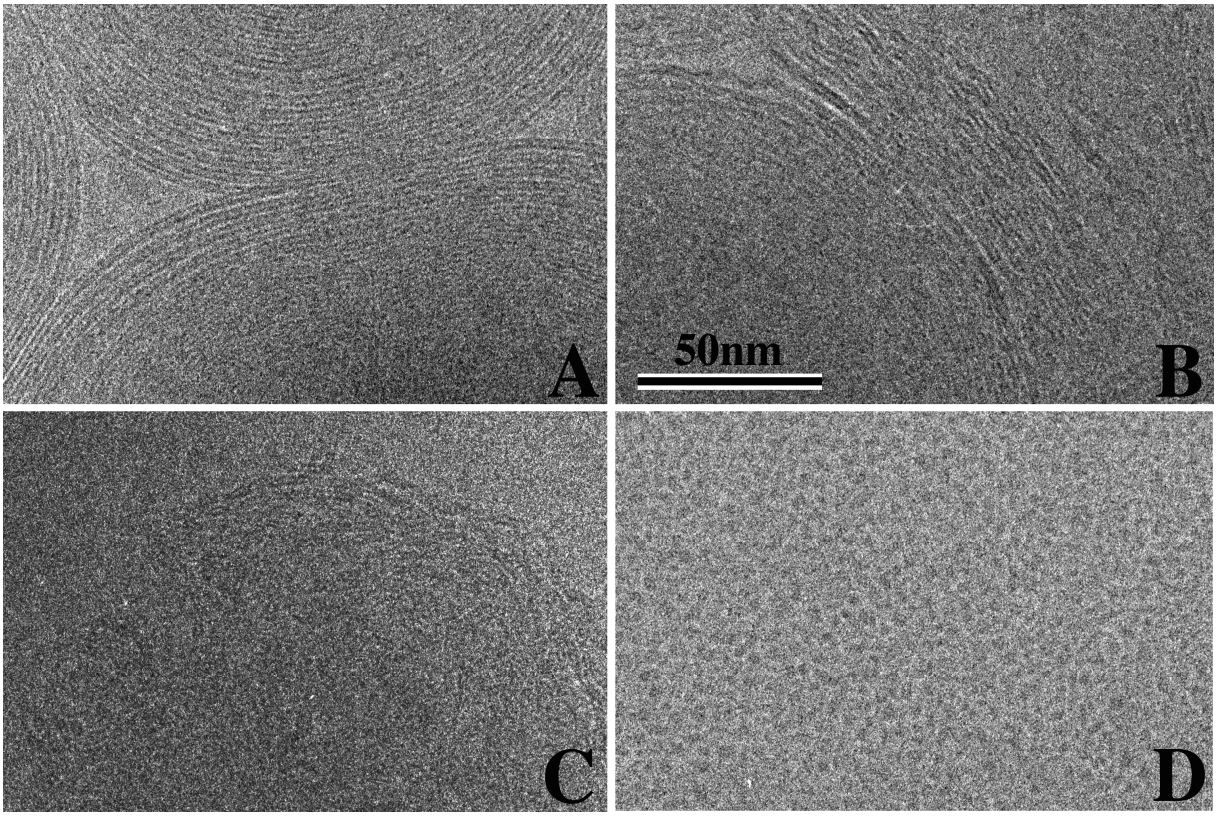

Figure 2 A-D: Enlarged views of membrane structures formed at different LPR, no protein (A), 300 (B), 100 (C) and 10 (D). Decreasing LPR correlates with increasing membrane distortion and a reduction of the membrane contrast. For LPR below 50, small particulate objects are detected that are referred as lipid micelles containing NS4B.

Overall effects of NS4B on lipid phases by various biophysical studies

DMPC has been extensively characterized [33] and constitutes a simple and appropriate system to assess the effect of a protein on the structure of membranes. At a water concentration above 20 % (weight / total weight), DMPC presents three temperature-dependant phases: (i) Below 14 °C, the aliphatic chains are stiff, arranged on a quasi-hexagonal lattice and tilted with respect to the normal to the lattice plan. This phase is generally referred as Lβ' (Luzzati, 1968). (ii) At 14-24 °C, the aliphatic chains have the same conformation as for Lβ', but the surface of the membrane is rippled, forming the Pβ' phase [33]. (iii) Above 24°C, the membrane flattens and the chains disorder, forming the Lα phase [34]. These three lamellar structures are observable in hydrated DMPC (30 % water) by their characteristic X-ray diffraction patterns at the appropriate temperatures (Figure 3 A-C). In particular, the complex, sharp reflection located around 4.2 Å, observed at 20 °C (Fig 3B), is replaced by a broad reflection centered around 4.6 Å when the temperature is increased above

24 °C - consistent with the gel-liquid crystalline transition of aliphatic chains. When NS4B was incorporated in the hydrated DMPC phase at an LPR of 300, both the low and high angle reflections broadened so that the phase transitions were difficult to detect (Figure 3 D). Similar patterns were obtained in the 10-30 °C temperature range (data not shown), demonstrating that NS4B greatly affects the structure of DMPC membranes and anneals the phase transitions of aqueous DMPC lamellae.

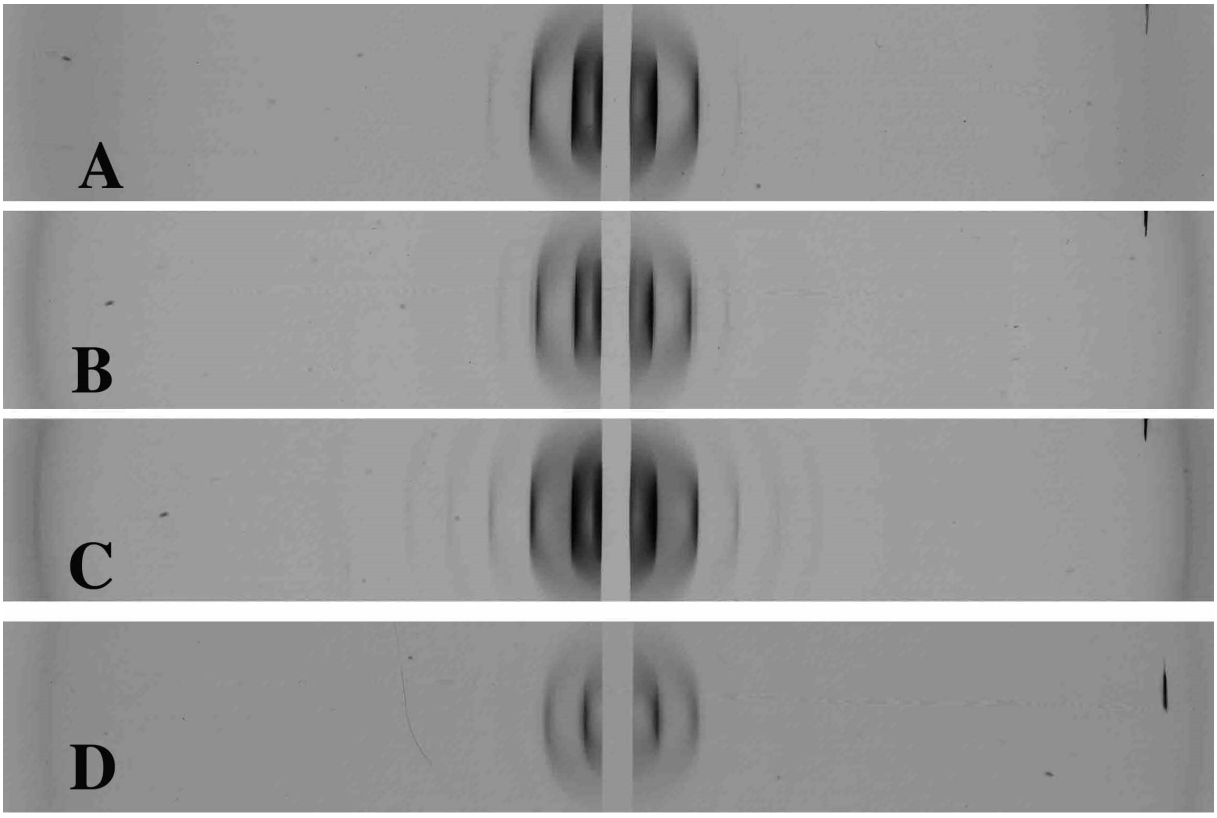

Figure 3: X-ray diffraction of NS4B and DMPC aqueous mixtures at different temperatures. All samples contain 30 % water. In A, B and C no protein is present. In D the LPR is equal to 100. The temperature is equal to 25°C in A, 20°C in B, 10°C in C and 20°C in D. While the pattern is sensitive to temperature for pure DMPC, it is similar for NS4B-DMPC mixture in the temperature range 10-30°C.

Membrane perforation and fusion activities of terminal peptides

To further investigate the molecular mechanism of NS4B-induced membrane disorganization, we investigated the effects of consensual N- and C-terminal amphipathic helices (AH1, AH2 and H2) on liposomes. The synthesized peptides are referred to as pepAH1, pepAH2 and pepH2. Due to its rather small length, the properties of H1 were not investigated. The effects

of the different peptides were analyzed using a fluorescent test on artificial membranes.

Liposomes containing high concentrations of carboxyfluorescein display reduced fluorescence intensity as a result of self-quenching. When the liposomes are disrupted the drug is released into the external medium, lowering its concentration and hence the degree of self-quenching, thereby increasing its fluorescence activity. This constitutes a simple test to investigate the membrane perforation properties of any compound. All three peptides, pepAH1, pepAH2 and pepH2, did indeed perforate liposomes (Figures 4 A and SI 4). The amplitude and rate of the fluorescence increase varied with peptide concentration. While the activity of pepH2 and pepAH2 were similar, the perforation activity of pepAH1 was five times lower. It should be noted that 1 mM pepH2 and pepAH2 exhibit an activity similar to 0.1 % Triton X-100 (v/v). None of these peptides disrupted red blood cell at physiological pH, and so the pore size could not be measured by hemolysis protection experiments.

In addition to perforation, peptides may also induce membrane fusion [35]. We tested this possibility by fluorescence resonance energy transfer between donor and acceptor fluorescent molecules associated with lipid. When liposomes marked with both fluorescent molecules are mixed with regular liposomes, peptides inducing membrane fusion lead to a greater distance between donor and acceptor - reducing the energy transfer rate and thus increasing the yield of fluorescence emitted by the donor (and decreasing that from the acceptor). As seen in Figure B, the addition of pepH2 to a mixture of regular and fluorescent liposomes led to an increase in donor fluorescence. This increase required the presence of both regular and fluorescent liposomes - it did not appear when pepH2 was added to fluorescent liposomes alone (violet trace in Figure 4 B). The increase did not arise from adsorption phenomena induced by the peptide, but resulted from the fusion of regular and fluorescent membranes. PepAH1 and pepAH2 did not show any fusion activity (data not shown); only pepH2 was thus further investigated.

Liposome fusion required a rather high concentration of peptide (> 1 μM). Indeed, the peptides are not soluble in water and only a small fraction can insert into membranes. Thus when NS4B-liposome samples were centrifuged through a sucrose density gradient, most of the peptides were found in the bottom fraction (Figure SI 5), while the peptides dissolved in water exhibited large aggregates as observed by dynamic light-scattering (data not shown). The large concentration of peptides necessary to affect liposome membrane can thus be attributed to their low solubility in water and not to the existence of different destabilization mechanisms for NS4B and pepH2.

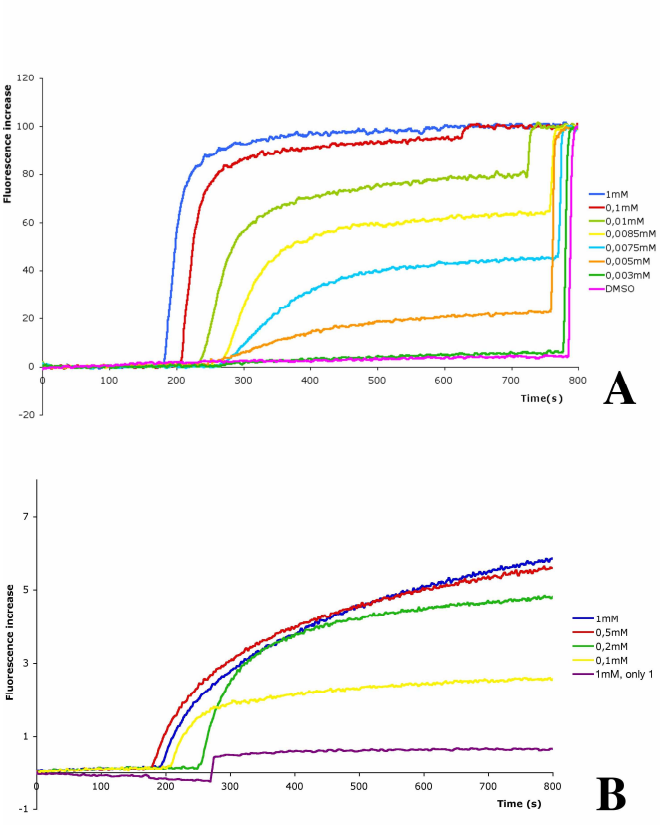

Figure 4: Perforation (A) and fusion (B) activities of pepH2. Perforation analysis was performed using pepH2 concentrations, in DMSO, of 1 (blue), 0.1(red), 0.01 (light green), 0.085 (yellow), 0.075 (light blue), 0.005 (orange), 0.003 (green), and 0 (pink) mM (for 0 mM, pure DMSO was added). Fusion experiments were carried out at pepH2 concentrations of 1 (blue, violet), 0.5 (red), 0.2 (greeen), and 0.1 (yellow) mM. In the absence of non-fluorescent lipids (violet), no fluorescence increase is observed.

Cryo-electron microscopy of liposomes in the presence of pepH2

Liposomes were visualized by cryo-EM, as spherical objects defined by a single bilayer. The apparent diameter of the liposomes was rather constant, with values generally less than 0.5 µm (Figure 5A). When several liposomes aggregate, the membranes keep their double-layered structure (figure 5A). Multi layered liposomes were rare. When pepH2 was added at a concentration of 25 µM, most liposomes aggregated (Figure 5 B). Many liposomes contained a second one - suggesting that the presence of the peptide lead to an invagination of the membrane and formation of an internal liposome (Figures 5B). PepH2 appears thus to have the capacity to transform liposome into double membrane vesicles by a mechanism that remains unknown. When the liposomes aggregated, the contrast of the interacting layers is reduced (Figure 5 B-D) and a succession of high and low densities is observed along the

centre. These two observations indicate a disorganization of the lipid polar head domains of the interacting bilayers, reflecting a reorientation of their aliphatic chains as a result of peptide insertion. Figure 6 shows enlarged views of interacting liposomes in absence (A) and presence (B) of pepH2. In presence of pepH2 the contrast of the interacting leaflets reduces in some areas. In addition, the aqueous medium between the liposomes completely disappears when NS4B is present. While these structures were absent in absence of NS4B, most aggregated liposomes displayed interacting layers with a reduced contrast. These structures suggest that the external liposome membranes have locally merged. The fact that the fusion area has conserved the thickness of two membranes suggests that the external leaflets fused in a succession of local hemi-fusion events. As the extent of each fused event is unknown, we referred this structure as arising from an hemi-fusion-like event.. Although most observed liposome interactions involved hemi-fusion-like event, full fusion events cannot be excluded. Although rare, pores were observed and displayed small diameter (Figure SI 6 A-B).

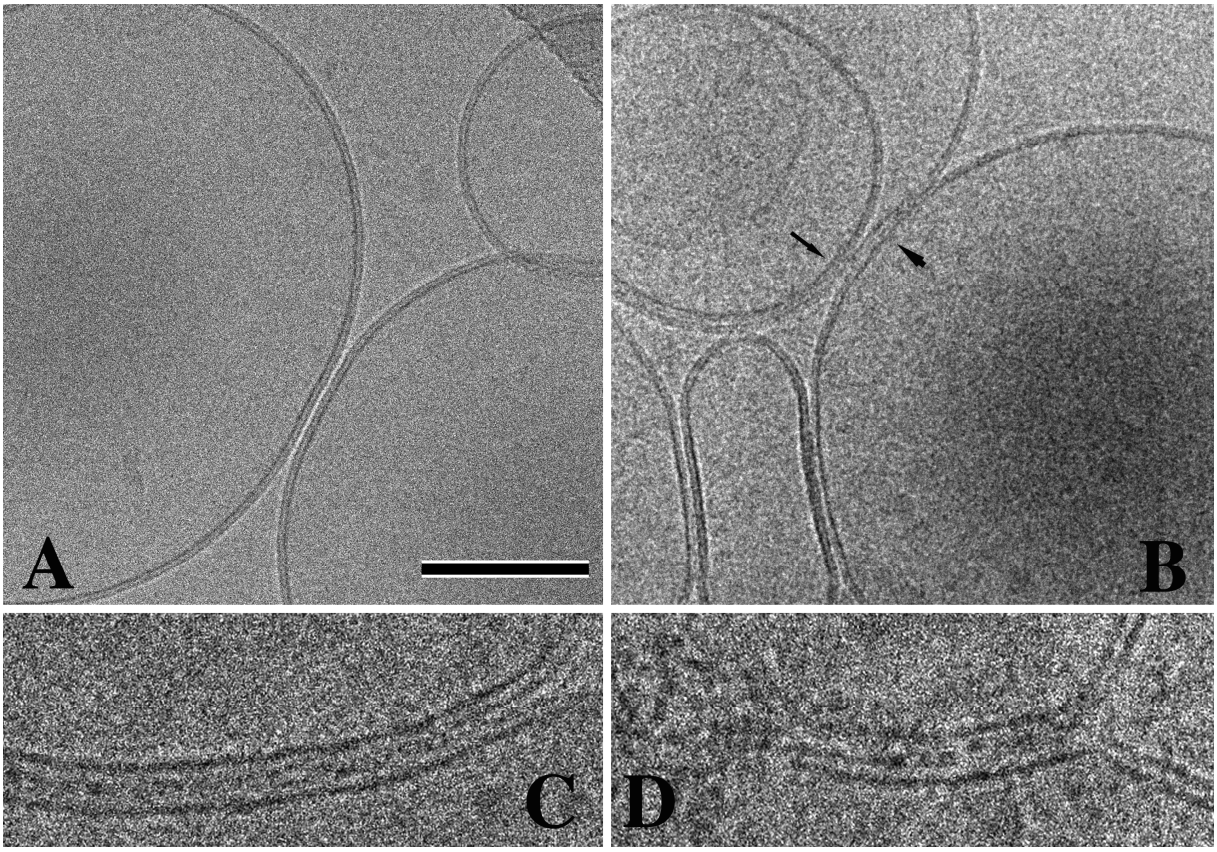

Figure 5: Effects of peptide H2 on liposomes. The scale bar represents 100 nm in A-B, and 33 nm in C-D. In the presence of pepH2 (B-D), liposomes have a strong tendency to aggregate; double concentric liposomes are also more often found. Some interacting membranes present a particular structure: the interacting membrane leaflets exhibit reduced contrast, and density variations appear within the external leaflets (C and D), indicating hemi-fusion-like events.

Reduced aqueous densities are observed between the interacting membranes in presence of pep H2 (C-D), in contrast to pure liposomes (A). Note that hemi-fusion appears between membranes of single-lamellar liposomes (large arrow in B) or between membranes of concentric liposomes (small arrow in B).

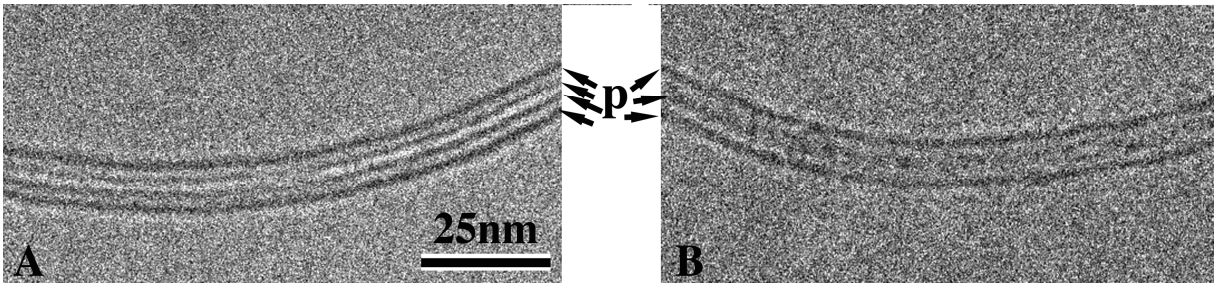

Figure 6: Images of the contact between liposome membranes in the absence (A) and presence (B) of peptide H2. Without pepH2, the low density arising from the external medium is clearly visible between the two bilayers (A); in the presence of pepH2, the lipid layers in contact have low contrast and the aqueous phase is no longer visible (B). The distance between the internal layers are identical, suggesting the existence of several hemi-fusion events. P indicates the polar heads; schematically, four distinct layers are seen in absence of pepH2 (A), while only three are present when pepH2 is present (B).

.

DISCUSSION

The aim of the present study was to investigate the specific contribution of NS4B to the membrane alterations associated with viral genome replication in HCV-infected cells. We first produced a recombinant full-length HCV NS4B by cell-free expression, in order to overcome the cyto-toxicity of NS4B upon cellular over-expression. Our protocol constitutes a fast and simple procedure for obtaining milligram quantities of this highly hydrophobic protein [30]. Several laboratories have already reported the purification of recombinant NS4B from different sources (Sf9 insect cells, bacteria), but detailed structural studies were hampered by low levels of expression [25, 27] or poor purity [26]. The high yield and purity of our preparation allowed for an in-depth biophysical study of the effects of NS4B on model membranes.

X-ray diffraction and electron microscopy studies demonstrate that the most important changes induced by NS4B concern the order within membranes. DMPC membranes regularly stack, forming lamellar phases at low water content or liposomes at higher water content. In the first case, the spacing between membranes is regular enough to give rise to rather sharp X-ray diffraction patterns, while concentric membranes are observed in cryoEM images for the second. When NS4B is present at LPR lower than 500, DMPC phases exhibit broadened X-ray diffraction patterns and disordered membrane stacks are observed by cryoEM. The membrane staking default in presence of NS4B appears as mainly due to membrane destabilization.the membrane disorder. While DMPC membranes are contiguous, NS4B induces the interruption of membranes, leading to the formation of membrane fragments and merged membranes. Fragmentation and merging of membranes decreases their homogeneity, potentially explaining the loss of cooperativity of the phase transitions.

NS4B, destabilizing and fragmenting liposomes, exhibits detergent-like properties. While this could be an artefact of incomplete detergent removal, at least two factors can exclude this hypothesis. Firstly, BioBead treatment was performed in optimal conditions (concentration, time course, temperature), under which DDM, the detergent used here, is totally absorbed [36]. Secondly, all our samples, liposomes and proteo-liposomes were reconstituted in the same conditions that led to the formation of liposomes when only pure lipid solutions were treated. The effect of NS4B on membranes is thus an intrinsic property of the protein.

The disorder introduced by NS4B on model membranes is similar but not identical to that observed *in-situ*. This difference is not surprising, and several studies have shown that multiple factors may influence the formation and morphology of MW (see [12]): lipid composition, recruitment of host-cell factors, the abundance of the different HCV NS

proteins, the formation kinetics of the HCV viral replication complex... The primary difference is the lipid composition in our model membranes. MW have been shown to be enriched in PI(4)P [37], and to be localized in cholesterol-rich lipid rafts [38], and these specific lipids can strongly influence the membrane architecture. Moreover, the local concentration of NS protein can also contribute to various morphologies of MW. Indeed, over-expression of NS proteins induced distinct membrane alterations, revealed by electron microscopy studies, and these membrane rearrangements change during the viral replication process [11, 39].

The domains corresponding to the C and N-terminal ends of NS4B have been proposed to be formed by amphipathic helices involved in membrane association: H2, AH1 and AH2 (H1, a small peptide, has not been studied). We confirmed that peptides corresponding to these regions of NS4B perforate liposome membranes. Cryo-EM images of perforated liposomes show pores where the internal aqueous medium is not resolved (Figure SI 6). The pore diameter is thus less than the dimension of the smallest object that can be visually detected by CryoEM, about 3 nm.Our data suggest that pepH2 is sufficient to induce membrane merging. Although fusion events could not be observed, their occurrence cannot be discarded. In the absence of tension on the membrane undergone by protein [40], the fusion process appears nevertheless blocked in hemi-fusion or at the step where an initial fusion pore is formed. The membrane fusion and perforation properties of NS4B reasonably explain its ability to disorder membranes, both *in vivo* and *in vitro*. While double membrane vesicles have been observed in MW [39, 41], such vesicles appear to be induced by the amphipathic domains of NS4B. All activities of NS4B on membranes could be explained by the presence of amphiphilic domains that insert into biological membranes. Because such domains are present in many proteins, the membrane activity of NS4B can thus be generalized - rearrangements of membranous compartments associated with the replication of positive RNA viruses may be due to the presence of amphiphilic domains. Due to their potential importance in the viral cycle, such amphiphilic domains are excellent targets for developing anti-viral agents.

In summary, we have shown that NS4B disorders biological membranes at different levels. Firstly, NS4B inhibits regular membrane stacking, impeding in particular their parallel arrangement. Secondly, while the boundaries of native membranes are continuous surfaces, the presence of NS4B introduces interruptions in the membrane and anastomosed network.

All studied peptides corresponding to the N- and C -terminal ends of NS4B perforate membranes. The peptide corresponding to H2 also induces membrane fusion and the formation of double membrane vesicles. Perforation and fusion of membranes induced by the

termini of NS4B, and by any exposed amphiphilic domains in general, are sufficient to explain the membrane disordering observed during formation of the virus replication complex.

MATERIAL AND METHODS

Materials

Detergents were purchased from Calbiochem (Brij35) and Interchim (DDM); all other chemicals were from Sigma. Solutions were filtered through 0.22 µm Millipore filters.

For fusion assays and liposome cryo-EM, peptides were dissolved in DMSO (Sigma) at 100 mM or lower. The maximum concentration of DMSO in the presence of lipid (Avanti) sample was 1 %.

Cell-free protein expression and purification

The encoding region of NS4B (genotype 1a, strain HCV H77C) was cloned between the NcoI and SmaI restriction sites of the pIVEX 2.3d and 2.4d vectors (5PRIME).The genome codes for a polyprotein containing 3011 amino acids (aa). NS4B starts at aa 1712 and is made up of 261 aa. These plasmids were designed to add a C- or N-terminal 6xHis tag respectively. Constructs were checked by sequencing, and plasmid DNA templates for cell-free production were purified using the Qiagen MidiPrep kit with an $OD_{260/280}$ >1.8. The plasmids was aliquoted and stored at -20 °C.

Cell-free expression was performed using the commercial 5PRIME kits RTS100 (small volume batch system BCF) and RTS500 (medium and preparative scale with continuous exchange CECF), according to the manufacturer's instructions, and the mixtures were incubated in the Eppendorf Thermomixer comfort device.

For initial screens, BCF reactions were performed in 50 µL reconstituted RTS100 *E.coli HY* lysate with 1 µg plasmidic DNA, supplemented with 1 % (w/v) Brij35, and incubated for 4 h at 30 °C and 660 rpm. The mixtures were loaded and separated on 12 % SDS-PAGE gels, then either stained with Coomassie blue or transferred onto nitrocellulose membranes for immunodetection with anti-His tag antibodies conjugated to peroxidase (Roche Applied Science).

For preparative-scale synthesis, CECF reactions were performed using 1 ml reconstituted RTS500 *E.coli HY* lysate with 15 µg plasmidic DNA, supplemented with 1 % (w/v) Brij35 per ml of reaction mix, and incubated for 20 h at 30 °C and 660 rpm.

At the end of expression, reaction solutions were pooled, diluted 1:10 in buffer A (50 mM Tris-HCl pH 7.5, 300 mM NaCl, 0.05% DDM), and incubated for 30 min at room temperature. After centrifugation for 30 min at 20,000 x g, the supernatant was loaded onto a Ni-NTA loaded HiTrap HP column (GE Healthcare) equilibrated with buffer A. Affinity chromatography was performed at 1 $mL.min^{-1}$ flow rate, with washing steps of 10 column

volumes of buffer A supplemented with 50 mM imidazol. Proteins were eluted with a linear (0.05-0.5 M) imidazol gradient in buffer A (3 column volumes). NS4B fractions were concentrated on Amicon Ultracel® -30kDa membrane concentrators (Millipore) and further purified on a gel-filtration column (Superdex 200, GE Healthcare), equilibrated with buffer B (50 mM Tris-HCl pH 7.5, 150 mM NaCl, 1 mM β-mercaptoethanol, 0.03% DDM), at a flow rate of 0.5 $ml.min^{-1}$.

Each of the purification steps was followed by Coomassie-blue-stained 12 % SDS-PAGE gel, according to the Laemmli method, to check sample purity.

Concentration of purified cell-free-expressed NS4B was determined by its absorbance at 280 nm, using extinction coefficient 39 440 M^{-1} cm^{-1}.

Proteoliposome reconstitution

To solubilize DMPC lipids, DDM was added in 50 mM Tris-HCl pH 7.5, 150 mM NaCl buffer at a detergent-to-lipid weight ratio of 2.5:1, followed by vigorous vortexing.

Purified NS4B was mixed with detergent-solubilized lipids at the desired final molar ratio; the final lipid concentration was 2 mg/ml. To remove the detergent, appropriate quantity of wet Bio-Beads (SM-2 Bio-Rad) were added every 30 min for 3 hours, with continuous stirring at room temperature to achieve the final Bio-Beads-to-detergent weight ratio of 40:1 (BioRad Instruction sheet). Following Bio-Bead removal, reconstituted proteoliposomes, in the presence or absence of NS4B, were then analyzed by electron microscopy.

Synthesis of NS4B terminal regions

Peptides corresponding to the N- and C-terminal amphipathic helices of NS4B (AH1 & AH2, and H2, respectively) were chemically synthesized as previously described [15, 42]. AH1, AH2 and H2 correspond to amino acids 1-34, 41-65 and 227-254 in the NS4B sequence, respectively, as follows:

AH1 SQHLPYIEQGMMLAEQFKQKALGLLQTASRHAEV

AH2 TNWQKLEVFWAKHMWNFISGIQYLA

H2 SDAAARVTAILSSLTVTQLLRRLHQWIS

Peptides were dissolved in DMSO to a concentration of 1 mM and kept at –20°C until use.

Liposome perforation assays

Liposomes containing carbofluorescein (CF) were prepared as previously described [43]. Briefly, phosphatidylcholine was suspended 10 mM NaCL and 10 Hepes buffer (pH 7.4). A concentrated solution of carbofluorescein was then added and the solution vortexed for at least 1 minute and then sonicated in a Besnson bath sonicator. Liposomes containing

fluorescein were separated from free carboflurescein by eluting the mixture through Sepharose column equilibrated with 150mM NaCl and 10 mM Hepes, pH 7.4.

The release of CF upon peptide addition was monitored as an increase in fluorescence at 520 nm, with excitation at 492 nm in a thermostatically controlled Perkin-Elmer LS50B spectrofluorimeter. 100 % CF release measured by addition of Triton X-100 at the end of the reaction. All fluorescence experiments were carried out at least three times.

Liposome fusion assays

Preparation of liposomes: 100 μg each of PE dissolved in organic solvents were mixed and dried *in vacuo.* To prepare fluorescent liposomes for fusion assays, 2.5 μg BODIPY 500/510 C_{12}-HPC (as fluorescence donor) and 5 μg BODIPY 530/550 C_5-HPC (as fluorescence acceptor) were added in the mixture before drying. The lipid film was resuspended in 0.2 ml buffer (150 mM NaCl, 5mM Tris-HCl pH 8), and the mixture was bath-sonicated for 20 minutes. Fluorescent and non-fluorescent liposomes were extruded through an Avanti extruder using 0.2 μm membranes; in general, 40 extruding passages were performed.

Fusion assay: fusion was assayed as previously described [44, 45]. Briefly, 10 μl fluorescent liposomes were mixed with 980 μl phosphate-citrate buffer at the required pH (prepared from 100 mM citric acid and 200 mM dibasic sodium phosphate solutions), in the cuvette of a thermostated Perkin-Elmer LS50B spectrofluorimeter. 10 μl non-fluorescent liposome suspension were added, followed by 10μl peptide solution, and the increase in BODIPY 500/510 C_{12}-HPC fluorescence was monitored continuously. Excitation was at 485 nm (slit width 5 nm) and emission was at 518 nm (slit width, 5 nm). The mixture was kept under continuous stirring during the experiment.

X-ray diffraction

Samples were prepared and the patterns recorded with a Guinier camera, as described previsouly [33].

Electron microscopy

Liposomes were prepared as for the perforation experiments at a concentration of 1 mg/ml. Peptide dissolved in DMSO at a concentration of 100mM was added was diluted 1000-100 times in the liposome sample. 1% DMSO did not change the liposome morphology (not shown).

Most samples were checked by conventional electron microscopy using the negative staining method. 3 μl sample were deposited on an airglow-discharged, carbon-coated grid. The

excess was blotted and the grid rinsed with 2 % phosphotungstic acid. Grids were observed in a Philips CM12 microscope operated at 80 kV, and images were recorded on Kodak electron image plates, which were then developed for 5 minutes in D19.

CryoEM was performed as described [46] using R2/2 quantifoil carbon film (Electron Microscopy Science). 3 µl of the sample were deposited on airglow-discharged quantifoil. The sample excess was blotted with a filter paper, and the grid plunged into liquid-nitrogen-cooled ethane. The grid was rapidly transferred and kept under liquid nitrogen. For observation, the grids were mounted in a 636 Gatan holder using its cryo-transfer device. The observations were made in a Technai 200 equipped with a field-emission gun. Images of the protein samples were typically recorded at 35,000 x magnification on SO163 films, which were developed for 12 minutes in D19 (Kodak). Each micrograph was recorded with about 20 electrons/A^2. Micrographs were scanned with a Nikon Coolscan 8000, at a resolution of 4000 dots per inch. Some images were low- and high-pass-filtered using Imagic [47]; these filters were set to optimize the observed contrast of membranes, typically 0.03 and 0.5 times the Nquist frequency, respectively. The images of pepH2 were recorded with a direct dtection camera (K2, Gatan) operated in movie mode. The images were aligned and summed as recommended by manufacturer. They were recorded at 29,000 magnification (pixel size 1.72Å) using a total dose less than 30 electrons/$Å^2$

ACKNOWLEGEMENTS

We thank Drs Thierry Meinnel and Félix Rey for their interest in this work that was supported by grants from Agence National contre le Sida et l'Hépatite C (ANRS), Agence National pour la Recherche (ANR). We also thank Dr. Andrew Pascal for reading the manuscript.

REFERENCES

[1] S. Miller, J. Krijnse-Locker, Modification of intracellular membrane structures for virus replication, Nat Rev Microbiol 6 (2008) 363-374.

[2] D. Lavanchy, The global burden of hepatitis C, Liver Int 29 Suppl 1 (2009) 74-81.

[3] Q.L. Choo, G. Kuo, A.J. Weiner, L.R. Overby, D.W. Bradley, M. Houghton, Isolation of a cDNA clone derived from a blood-borne non-A, non-B viral hepatitis genome, Science 244 (1989) 359-362.

[4] D. Moradpour, F. Penin, Hepatitis C virus proteins: from structure to function, current topics in microbiology and immunology 369 (2013) 113-142.

[5] R. Gosert, D. Egger, V. Lohmann, R. Bartenschlager, H.E. Blum, K. Bienz, D. Moradpour, Identification of the hepatitis C virus RNA replication complex in Huh-7 cells harboring subgenomic replicons, Journal of virology 77 (2003) 5487-5492.

[6] D. Egger, B. Wolk, R. Gosert, L. Bianchi, H.E. Blum, D. Moradpour, K. Bienz, Expression of hepatitis C virus proteins induces distinct membrane alterations including a candidate viral replication complex, Journal of virology 76 (2002) 5974-5984.

[7] U. Pfeifer, R. Thomssen, K. Legler, U. Bottcher, W. Gerlich, E. Weinmann, O. Klinge, Experimental non-A, non-B hepatitis: four types of cytoplasmic alteration in hepatocytes of infected chimpanzees, Virchows Arch B Cell Pathol Incl Mol Pathol 33 (1980) 233-243.

[8] M. Lundin, M. Monne, A. Widell, G. Von Heijne, M.A. Persson, Topology of the membrane-associated hepatitis C virus protein NS4B, Journal of virology 77 (2003) 5428-5438.

[9] D. Moradpour, R. Gosert, D. Egger, F. Penin, H.E. Blum, K. Bienz, Membrane association of hepatitis C virus nonstructural proteins and identification of the membrane alteration taht harbors the viral replication complex, Antiviral Re. 60 (2003) 103-109.

[10] H. Tang, H. Grisé, Cellular and molecular biology of HCV infection and hepatitis, Cli. Sci. 117 (2009) 49-65.

[11] G. Alvisi, V. Madan, R. Bartenschlager, Hepatitis C virus and host cell lipids: An intimate connection, RNA Biol. 8 (2011) 258-269.

[12] S. Salloum, A.W. Tai, Treating hepatitis C infection by targeting the host, Transl. Res. 159 (2012) 421-429.

[13] T. Hügle, F. Fehrmann, E. Black, M. Kohara, H.G. Kraüsslich, C.M. Rice, H.E. Blum, D. Moradpour, The hepatitis C virus non integral protein 4B is an integral endoplasmic reticulum membrane protein, Virology 284 (2001) 70-81.

[14] M. Elazar, P. Liu, C.M. Rice, J.S. Glenn, An N-terminal amphipathic helix in hepatitis C virus (HCV) NS4B mediates membrane association, correct localization of replication complex proteins, and HCV RNA replication, Journal of virology 78 (2004) 11393-11400.

[15] J. Gouttenoire, R. Montserret, A. Kennel, F. Penin, D. Moradpour, An amphipathic alpha-helix at the C terminus of hepatitis C virus nonstructural protein 4B mediates membrane association, Journal of virology 83 (2009) 11378-11384.

[16] J. Gouttenoire, V. Castet, R. Montserret, N. Arora, V. Raussens, J.M. Ruysschaert, E. Diesis, H.E. Blum, F. Penin, D. Moradpour, Identification of a novel determinant for membrane association in hepatitis C virus nonstructural protein 4B, Journal of virology 83 (2009) 6257-6268.

[17] N.-J. Cho, H. Dvory-Sobol, L. Choongho, S.-J. Cho, P. Bryson, M. Masek, M. Elazar, C.W. Frank, J.S. Glenn, Identification of a class of HCV inhibitors directed against the

nonstructural protein NS4B, Sci. Transl. Med. 20 (2010) 1-17.
[18] J. Guillen, Gonzalez-Alvarez, J. A. Villalain, A membranotropic region in the C-terminal domain of hepatitis C virus protein NS4B Interacyion with membranes, BIochimica et Biophysica Acta 1798 (2010) 327-337.
[19] M.F. Palomares-Jerez, J. Villalain, membrane interaction of segment H1 (NS4BH1) from hepatitis C virus non-structural protein 4B, BIochimica et Biophysica Acta 1808 (2011) 1219-1229.
[20] M.F. Palomares-Jerez, H. Nemesio, H.G. Franquelim, M.A. Castanho, J. Villalain, N-terminal AH2 segment of protein NS4B from hepatitis c virus. Binding to and interaction with model biomembranes, Biochemical and Biophysical Acta 182 (2013) 138-152.
[21] M.F. Palomares-Jerez, H. Nemesio, J. Villalain, Interactions with membranes of the full C-teminal domain of protein NS4B from Hepatitis C virus, BIOchimica et Biophysica Acta 1818 (2012) 2536-2549.
[22] M. Lundin, H. Lindstrom, C. Gronwall, M.A. Persson, Dual topology of the processed hepatitis C virus protein NS4B is influenced by the NS5A protein, The Journal of general virology 87 (2006) 3263-3272.
[23] G.Y. Yu, K.J. Lee, L. Gao, M.M. Lai, Palmitoylation and polymerization of hepatitis C virus NS4B protein, Journal of virology 80 (2006) 6013-6023.
[24] J. Gouttenoire, F. Penin, D. Moradpour, Hepatitis C virus nonstructural protein 4B: a journey into unexplored territory, Reviews in medical virology 20 (2010) 117-129.
[25] S. Einav, M. Elazar, T. Danieli, J.S. Glenn, A nucleotide binding motif in hepatitis C virus (HCV) NS4B mediates HCV RNA replication, Journal of virology 78 (2004) 11288-11295.
[26] A.A. Thompson, A. Zou, J. Yan, R. Duggal, W. Hao, D. Molina, C.N. Cronin, P.A. Wells, Biochemical characterization of recombinant hepatitis C virus nonstructural protein 4B: evidence for ATP/GTP hydrolysis and adenylate kinase activity, Biochemistry 48 (2009) 906-916.
[27] S. Einav, D. Gerber, P.D. Bryson, E.H. Sklan, M. Elazar, S.J. Maerkl, J.S. Glenn, S.R. Quake, Discovery of a hepatitis C target and its pharmacological inhibitors by microfluidic affinity analysis, Nat Biotechnol 26 (2008) 1019-1027.
[28] H. Dvory-Sobol, P.S. Pang, J.S. Glenn, The future of HCV theraoy: NS4N as antiviral target, Viruses 2 (2010) 2481-2492.
[29] D. Paul, I. Romero-Brey, J. Gouttenoire, S. Stoitsova, J. Krijnse-Locker, D. Moradpour, R. Bartenschlager, NS4B self-interaction through conserved C-terminal elements is required for the establishment of functional hepatitis C virus replication complexes, Journal of virology 85 (2011) 6963-6976.
[30] M.-L. Fogeron, V. Jirasko, S. Oenzel, D. Paul, R. Montserret, C. Danis, D. Lacabonne, A. Badillo, j. Gouttenoire, D. Moradpour, R. Nartenschlager, F. Penin, B.H. Meir, A. Böckmann, Cell-free expression, purification, and membrane reconstitution
for NMR studies of the nonstructural protein 4B from hepatitis C
virus, J. Biomol. NMR 65 (2016) 87-98.
[31] P. Richard, J.L. Rigaud, P. Graber, Reconstitution of CF0F1 into liposomes using a new reconstitution procedure, European journal of biochemistry / FEBS 193 (1990) 921-925.
[32] J. Lepault, F. Pattus, N. Martin, Cryo-electron microscopy of artificial biological membranes, Biochimica et biophysica Acta (BBA) - Membranes 820 (1985) 315-318.
[33] A. Tardieu, V. Luzzati, F.C. Reman, Structure and polymorphism of the hydrocarbon chains of lipids: a study of lecithin-water phases, J Mol Biol 75 (1973) 711-733.
[34] V. Luzzati, X-ray diffraction studies of lipid-water system, Acad. Press 1968.

[35] S.A. Wharton, S.R. Martin, R.W. Ruigrok, J.J. Skehel, D.C. Wiley, Membrane fusion by peptide analogues of influenza virus haemagglutinin, The Journal of general virology 69 (Pt 8) (1988) 1847-1857.
[36] J.L. Rigaud, G. Mosser, J.J. Lacapere, A. Olofsson, D. Levy, J.L. Ranck, Bio-Beads: an efficient strategy for two-dimensional crystallization of membrane proteins, Journal of structural biology 118 (1997) 226-235.
[37] N.Y. Hsu, v. Ilnytska, F.J., G. Belov, M. Santiana, Y.H. Chen, P.M. Takvorian, C. Pau, H. van der Schaar, N. Kaushik-Basu, T. Balla, C.E. Cameron, E. Ehrenfeld, F.J. van Kuppeveld, N. Altan-Bonnet, Viral reorganization of the secretory pathway generates distinct organelles for RNA replication, Cell 141 (2010) 799-811.
[38] H. Aizaki, K.J. Lee, V.M. Sung, H. Ishiko, M.W. Lai, Characterization of the hepatitis C virus RNA replication complex associated with lipid rafts, Virolgy 324 (2004) 450-461.
[39] I. Romero-Brey, A. Merz, A. Chiramel, J.Y. Lee, P. Chianda, U. Haselman, R. Santarella-Mellwig, A. Habermann, S. Hoppe, S. Kallis, P. Walther, C. Antony, J. krijnse-Locker, R. Bartensclager, Three-dimensional architecture and biogenesis of membrane structure associated with hepatitis C virus replication, Plos pathogene 8 (2012) 1-21.
[40] S. Libersou, A.A.V. Albertini, M. Ouldali, V. Maury, C. Maheu, H. Raux, F. de Haas, S. Roche, S. Gaudin, J. Lepault, Distinct structural rearrangements of the VSV glycoprotein drive membrane fusion, Journal of Cell Biology 191 (2010) 199-210.
[41] D. Paul, S. Hoppe, G. Saher, J. Krijnse-Locker, R. Bartenschlager, Morphological and biochemical characterization of the membranous hepatitis C virus teplication compartment, J. Virol. 87 (2013) 10612-10627.
[42] J. Gouttenoire, R. Montserret, D. Paul, R. Castillo, S. Meister, R. Bartenschlager, F. Penin, D. Moradpour, Aminoterminal amphipathic alpha-helix AH1 of hepatitis C virus nonstructural protein 4B possesses a dual role in RNA replication and viral production, Plos pathogene 10 (2014) 1-17.
[43] P. Nandi, A. Charpilienne, J. Cohen, Interaction of rotavirus particles with liposomes, Journal of virology 66 (1992) 3363-3367.
[44] V.S. Malinin, M.E. Haque, B.R. Lentz, The rate of lipid transfer during fusion depends on the structure of fluorescent lipid probes: a new chain-labeled lipid transfer probe pair, biochemistry 40 (2001) 8292-8299.
[45] S. Roche, Y. Gaudin, Evidence that rabies virus forms different kinds of fusion machines with different pH thresholds for fusion, J. Virol. 78 (2004) 8746-8752.
[46] J. Lepault, F.P. Booy, J. Dubochet, Electron microscopy of frozen biological suspensions, Journal of microscopy 129 (1983) 89-102.
[47] M. van Heel, G. Harauz, E.V. Orlova, R. Schmidt, M. Schatz, A new generation of the IMAGIC image processing system., J. Struct. Biol. 116 (1996) 17-24.
[48] G.-Y. Yu, K.J. Lee, L. Gao, M.M. Lai, Palmitoylation and polymerization of hepatitis C virus NS4B protein, J. Virol. 80 (2006) 6013-6023.
[49] N. Sreerama, R.W. Woody, On the analysis of membrane protein circular dichroism spectra, Protein Sci. 13 (2004) 100-112.

+NS4B+

?

+

NS4B pepH2

+